ELSEVIER

Structure and dynamics of 6-Hydroxymethyl-7,8-dihydropterin pyrophosphokinase

Honggao Yan,* Jaroslaw Blaszczyk,† Bing Xiao,† Genbin Shi,* and Xinhua Ji†

**Department of Biochemistry, Michigan State University, East Lansing, MI, USA*
†Program in Structural Biology, National Cancer Institute-FCRDC, Frederick, MD, USA

Folates are essential for life. Unlike mammals, most microorganisms must synthesize folates de novo. 6-Hydroxymethyl-7,8-dihydropterin pyrophosphokinase (HPPK) catalyzes pyrophosphoryl transfer from ATP to 6-hydroxymethyl-7,8-dihydropterin (HP), the first reaction in folate pathway, and therefore, is an ideal target for developing novel antimicrobial agents. Because of its small size and high thermal stability, E. coli HPPK is also an excellent model enzyme for studying the mechanisms of enzymatic pyrophosphoryl transfer. We have determined the crystal structures of HPPK in the unligated form and in complex with HP, two Mg^{2+} ions, and AMPCPP (an ATP analog that inhibits the enzymatic reaction). Comparison of the two crystal structures reveals dramatic conformational changes of three flexible loops and many side chains and possible roles of the active site residues. © *2001 by Elsevier Science Inc.*

Keywords: antimicrobial agent, folate, HPPK, pterin, pyrophosphokinase, conformational change, protein flexibility, NMR spectroscopy, X-ray crystallography

INTRODUCTION

Rapidly increasing antibiotic resistance in recent years has rendered the current antibiotics ineffective for treating many microbial infections, resulting in a worldwide health care crisis.[1–5] According to a 1999 World Health Organization report,[6] infectious diseases are the leading causes of death and the main causes of premature death in the world. The crisis is further aggravated by the fact that most of new antibiotics are chemical modifications of the basic structures of existing antimicrobial agents against old targets and thus less effective against widespread antibiotic resistance. Therefore, new targets for developing novel antimicrobial agents are urgently needed for combating the antibiotic crisis. 6-Hydroxymethyl-7,8-dihydropterin pyrophosphokinase (HPPK) catalyzes the transfer of pyrophosphate from ATP to 6-hydroxymethyl-7,8-dihydropterin (HP), the first reaction in the folate biosynthetic pathway.[7] Folate cofactors are essential for life.[8] Mammals have an active transport system for deriving folates from their diet. In contrast, most microorganisms must synthesize folates de novo because they lack the active transport system. Therefore, the folate biosynthetic pathway is an ideal target for developing antimicrobial agents. Inhibitors of dihydropteroate synthase [9] and dihydrofolate reductase,[10] the second and fourth enzymes in the folate pathway, are currently used as antibiotics for treating many infectious diseases. HPPK represents a new target in a biosynthetic pathway that has been proven effective for the development of antimicrobial agents. Because of its small size and high thermal stability,[11,12] HPPK is also an excellent model enzyme for studying the mechanisms of enzymatic pyrophosphoryl transfer. Although the mechanisms of many kinases that catalyze monophosphoryl transfer have been extensively characterized, little is known about the mechanisms of pyrophosphokinases.[13] Despite the significance of HPPK as a new target for developing antimicrobial agents and a model system for studying the enzymology of pyrophosphoryl transfer, active studies of HPPK have just begun,[14–18] probably due to the low abundance of HPPK in the cell.[11] Very recently, four high-resolution crystal structures of HPPK have been reported. We have determined the crystal structures of apo-HPPK from *E. coli* at 1.5-Å resolution[14] and the complex of the HPPK with HP, AMPCPP (an analog of ATP), and two Mg^{2+} ions (HPPK · HP · MgAMPCPP) at 1.25-Å resolution.[19] Hennig et al. have reported the crystal structure of *H. influenzae* HPPK in complex with an HP analog at 2.1-Å resolution.[16] Stammers et al. have reported the crystal structure of *E. coli* HPPK in complex with another HP analogue, ATP and two Mg^{2+} ions at 2.0 Å resolution.[17] Of the three complex structures, HPPK · HP · MgAMPCPP most closely mimic the ternary complex.[19] Here, we compare the crystal structures of apo-HPPK and HPPK ·

Corresponding author: H. Yan, Department of Biochemistry, Michigan State University, East Lansing, MI 48824, USA.

E-mail address: yanh@pilot.msu.edu (H. Yan)

655 Avenue of the Americas, New York, NY 10010
1093-3263/01/$–see front matter
PII 1093-3263(00)00135-2

HP · MgAMPCPP and describe the roles of active site residues in catalysis and induced fit.

The Structure of apo-HPPK

The crystal structure of *E. coli* HPPK at 1.5-Å resolution was solved using MAD data collected from crystals containing selenomethionine (SeMet).[14] HPPK has a three-layered $\alpha\beta\alpha$ fold formed by six β-strands and four α-helices in the sequence $\beta1$-$\alpha1$-$\beta2$-$\beta3$-$\alpha2$-$\beta4$-$\beta5$-$\beta6$-$\alpha3$-$\alpha4$ (Figure 1a). In the center, the six β-strands are organized into an antiparallel β-sheet ($\beta2$, $\beta3$, $\beta1$, and $\beta4$) and a β-hairpin ($\beta6$ and $\beta5$). The angle between the adjacent $\beta4$ and $\beta6$ is ~70°. On each side of the central β-structure, there are two α-helices. The structural motif $\beta1$-loop-$\alpha1$ (residues 8 to 15) assumes two distinct conformations with a population ratio of 0.54:0.46. The fold of the HPPK molecule creates a valley that is approximately 26-Å long, 10-Å wide, and 10-Å deep (Figure 1b). The valley starts from a V-shaped cleft between $\beta6$ and the continuing loop (residues 110 to 116), runs along the $\alpha2$ helix and across the face of the four-stranded β-sheet, and ends at the carboxyl-terminal loop. Three flexible loops, $\beta2$-$\beta3$ (residues 43 to 53 with higher-than-average temperature factors), $\beta1$-$\alpha1$ (residues 8 to 15 with two conformations), and $\alpha2$-$\beta4$ (residues 82 to 92 with higher than average temperature factors) form one wall of the valley. The other wall of the valley is relatively rigid and is constructed by the structural motif $\beta6$-loop-$\alpha3$, where residues Val113, Pro114, Met118, Met124, Leu125, Trp126, Pro127, Leu128, and Phe129 participate in the formation of the protein's hydrophobic core. Thirteen strictly conserved residues among 11 HPPK sequences (Gly8, Asn10, Gln50, Asn55, Glu77, Arg82, Arg92, Asp95, Asp97, Leu111, Pro114, His115, and Arg121 in Figure 2 and Figure 3) are located in three regions of the valley. The flexible wall contains Gly8, Asn10, Gln50, Arg82, and Arg92, whereas Leu111, Pro114, and His115 are located in the rigid wall. In the bottom of the valley reside Arg121, Asn55, Glu77, Asp95, and Asp97. Glu77, Asp95, and Asp97 cluster in the middle portion of the valley, resulting in an area with concentrated negative charges. Therefore, the valley is most likely the active center where the two substrates (ATP and HP) and the Mg^{2+} ion bind. To identify the binding sites for ATP and HP, ^{1}H-^{15}N HSQC NMR spectra of HPPK were obtained with and without the presence of ATP or 6-hydroxymethylpterin (a competitive inhibitor of the substrate HP). The sequential resonance assignments of unliganded HPPK and its complex with magnesium adenylyl (β,γ-methylene)diphosphonic acid (a competitive inhibitor of the substrate ATP) have been achieved by three-dimensional double and triple resonance spectroscopy using uniformly ^{15}N- and $^{15}N/^{13}C$-labeled HPPK samples, including three-dimensional HNCACB, CBCA(CO)NH, HCCH-TOCSY and ^{15}N-edited NOESY-HSQC experiments.[15] The binding of 6-hydroxymethylpterin caused significant changes in the chemical shifts of ~15% of the backbone amide resonances. Of these backbone amides, most are localized in a region that contains the conserved residue Asn55 and the rest are localized in a region that contains the conserved residue Leu111. Therefore, the region of the valley that contains Asn55 is most likely the binding site for the substrate HP. Because 6-hydroxymethylpterin also binds to the ATP site but with a

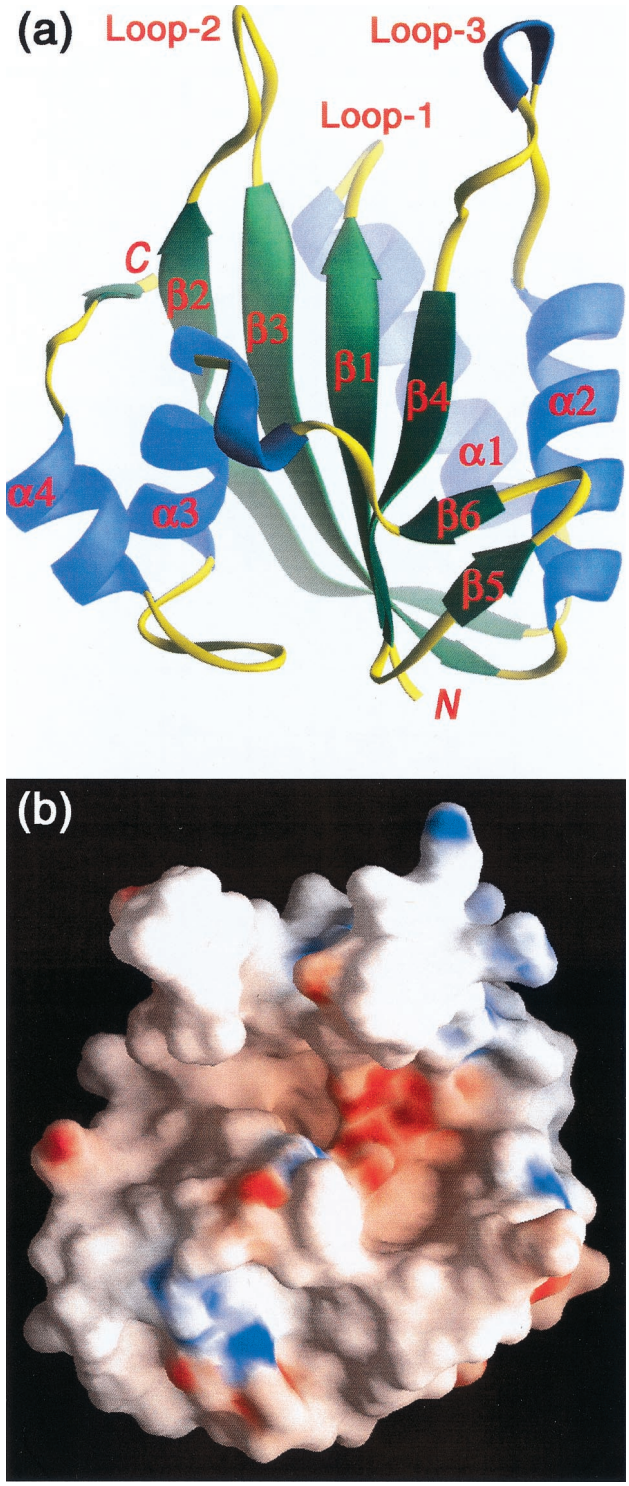

Figure 1. (a) The fold of apo-HPPK. The α-helices and consecutive β-turns are represented as blue spirals, β-strands as green arrows, and loops as yellow pipes. The illustration was prepared using RIBBONS.[20] (b) The van der Waals (vdw) surface representation of HPPK. According to electrostatic potential, the vdw surface is colored as blue for positive and red for negative. The illustration was prepared using GRASP.[21]

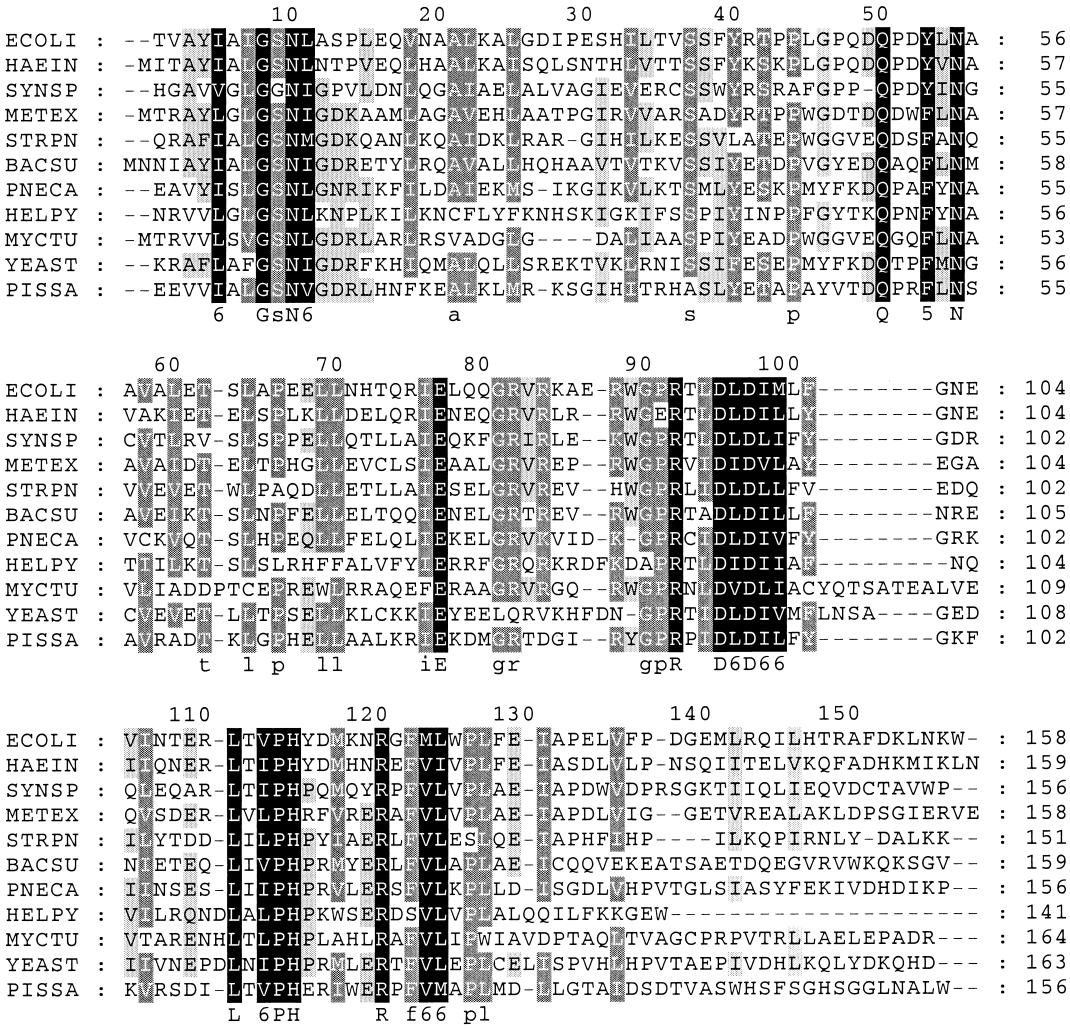

Figure 2. Amino acid sequence alignment of 11 HPPKs. The numbering at the top of the alignment is that of E. coli *HPPK. The conserved residues are highlighted in black. The strictly conserved residues are indicated with capital letters at the bottom of the alignment, and the highly conserved residues with lower case letters and numbers. The nomenclature of the HPPKs are as follows: ECOLI,* E. coli*; HAEIN,* Haemophilus influenzae*; SYNSP,* Synechocystis sp.*; METEX,* Methylobacterium extorquens; *STRPN,* Streptococcus pneumoniae*; BACSU,* Bacillus subtilis*; PNECA,* Pneumocystis carinii*; HELPY,* Helicobacter pylori*; MYCTU,* Mycobacterium tuberculosis*; YEAST,* Saccharomyces cerevisiae*; and PISSA,* Pisum sativum. *To save space, all HPPKs except ECOLI, HAEIN, and METEX are truncated at N-terminus, C-terminus, or both termini.*

much lower affinity than to the HP site, the region of the valley that contains the conserved residue Leu111 is most likely the binding site for ATP. Indeed, the binding of ATP caused significant changes in the chemical shifts of many backbone resonances in this region. Surprisingly, the binding of ATP also caused significant changes in the chemical shifts of many backbone amide resonances in the tentative HP-binding site. Because ATP has only one binding site in HPPK, the shift changes of the residues in the HP-binding site are probably due to conformational changes induced by the binding of ATP. The fact that the side chains of several conserved residues (Gln50, Arg82 and Arg92) point away from the active center (Figure 3) also suggests that catalysis by HPPK require induced conformational changes to bring the functional groups of these conserved residues to the active center.

The Structure of HPPK · HP · MgAMPCPP

The assignment of the substrate binding sites has been confirmed by the crystal structures of HPPK in complex with substrates or substrate analogs,[16,17,19] including HPPK · HP · MgAMPCPP which closely mimic the ternary complex of HPPK.[19] The interactions between HPPK and the bound HP, two Mg^{2+} ions and AMPCPP are shown in Figure 4. Nine residues are involved in HP binding: Gly8, Thr42, Pro43, Leu45, Tyr53, Asn55, Trp89, Asp95 and Phe123. HP forms six hydrogen bonds with residues Thr42, Pro43, Leu45, and Asn55, which saturate the hydrogen bond donors and acceptors of HP on positions 1, 2, 3, 4, and 8. The hydrogen bond donor NH of HP at position 5 interacts with Wat1, a coordination water of Mg2, and Wat2 is within the hydrogen bond distance of the Asp95 side chain and the >C═O group at position 4 of

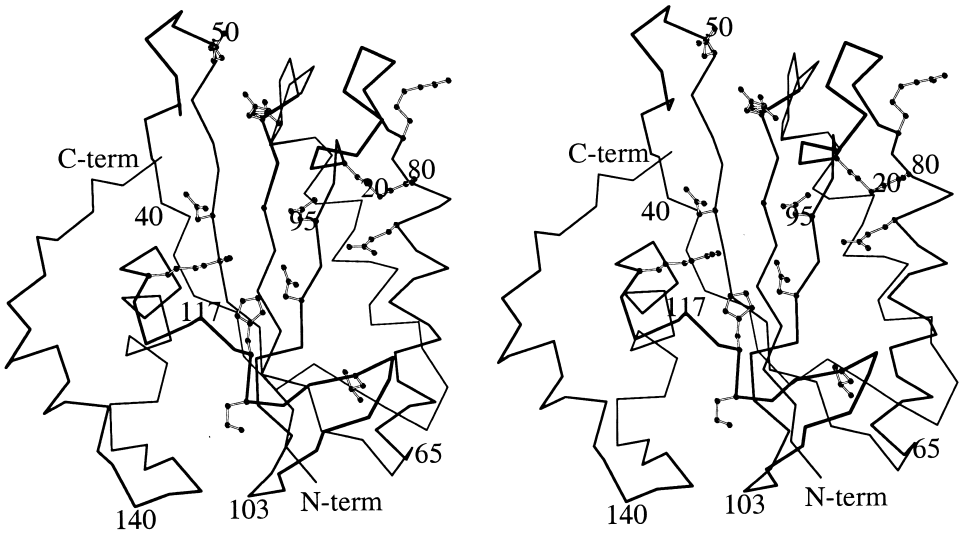

Figure 3. Stereo view of the Cα-trace of apo-HPPK. The sidechains of the 13 strictly conserved residues among 11 HPPKs are shown as ball-and-stick models. The illustration was prepared using MOLSCRIPT.[22]

HP. Hydrophobic interactions are provided by Gly8, Leu45, Tyr53, Trp89, and Phe123. The distance from the Cα atom of Gly8 to the ND2 atom of Asn55 is 3.6 Å and that to the HP carbonyl at position 4 is 4.3 Å. Any other residue at position 8 would inhibit HP binding for at least two reasons: it could prevent the conformational change of N55, a key residue for HP binding, and it could interfere HP binding simply via steric interactions. Two Mg^{2+} ions are found in the ternary complex and both are six-coordinated. Sharing a β-oxygen, Mg1 bridges the α- and β-phosphate groups and Mg2 links the β- and γ-phosphate groups. The two Mg^{2+} ions also share the side chain oxygen atoms of Asp95 and Asp97. The fifth and sixth coordination of Mg1 are provided by water molecules Wat3 and Wat4, whereas the fifth and sixth coordination of Mg2 are offered by the hydroxyl group of HP and Wat1. The resulting distance between the hydroxyl oxygen and the β-phosphorus is 3.2 Å, suggesting that the pyrophosphoryl transfer reaction has at least some associative character in the transition state. Twelve residues are involved in the binding of AMPCPP: Gln74, Glu77, Arg84, Arg88, Trp89, Arg92, Ile98, Arg110, Thr112, His115, Tyr116, and Arg121, among which Glu77, Arg92, His115, and Arg121 are conserved for 11 HPPKs. For Ile98, Arg110, and Thr112, the functional groups involved in AMPCPP binding are amides and/or carbonyls. Therefore, the side-chain nature of these three residues is irrelevant. The γ-phosphate group of AMPCPP is tethered by the side chains of His115, Tyr116, and Arg121, whereas the β- and α-phosphate groups form hydrogen bonds with the guanidinium groups of Arg92 and Arg84. Glu77 interacts with α-phosphate via a water molecule (Wat5). The ribose forms hydrogen bonds with the side chain of Gln74 and the carbonyl group of Arg110. The backbone amide and carbonyl groups of Ile98 and Thr112 are responsible for the recognition of the adenine moiety.

Induced Fit in HPPK

Indeed, the binding of HP and MgAMPCPP induces dramatic conformational changes in HPPK. If the apo-protein looks like a half-closed right hand (Figure 1b), the ternary complex appears to be a tightly closed fist (not shown). The most significant conformational differences reside in three flexible loops. In apo-HPPK, Loop-1 assumes two conformations with almost equal probabilities, whereas in the ternary complex, it has one well-defined conformation. Loops 2 and 3 move in to close the catalytic center (Figure 5a). Four of the 13 conserved residues are located in the three flexible loops: Asn10 in Loop-1, Gln50 in Loop-2, and Arg82 and Arg92 in Loop-3. The functional roles of Asn10 and Gln50 are revealed by the structure comparison of apo-HPPK and the ternary complex. In apo-HPPK, Loop-1 has two conformations and, therefore, Asn10 has two positions. Gln50 is located in Loop-2 and is therefore far from the active center. All three loops in apo-HPPK are very dynamic and the only significant linkage between the three loops is the electrostatic interaction between side chains Asn10 and Arg84 (Figure 3). However, in HPPK · HP · MgAMPCPP (Figure 5b), Asn10 and Gln50 become centers for the formation of a hydrogen bond network. Six hydrogen bonds are formed between the side chains of Asn10 and Gln50 and the backbone amide and/or carbonyl groups of Pro47, Trp89, Pro91, and Arg92. This network couples all three flexible loops and helps to stabilize the complex and seal the active center where the pyrophosphoryl transfer occurs. Upon substrate binding, the Cα atoms of Asn10, Pro47, Gln50, Arg84, Trp89, Pro91, and Arg92 shift 1.2, 8.1, 3.8, 6.2, 7.9, 4.2, and 2.5 Å, respectively. The conformational changes of the three loops and these residues are dramatic, resulting in the closure of the HP-binding pocket and the catalytic center and the direct interactions between the guanidinium groups of Arg84 and Arg92 and the bound nucleotide. Among the residues that interact with HP, Gly8 and Phe123 are the only residues that do not undergo significant positional and conformational changes. Residues Asn55 and Asp95 undergo conformational change via a rotation about the Cα-Cβ bond by approximately 23° and 80°, respectively. Residues Thr42, Pro43, and Tyr53 shift their positions toward bound HP by approximately 0.5, 2.0, and 1.5 Å, respectively. The most

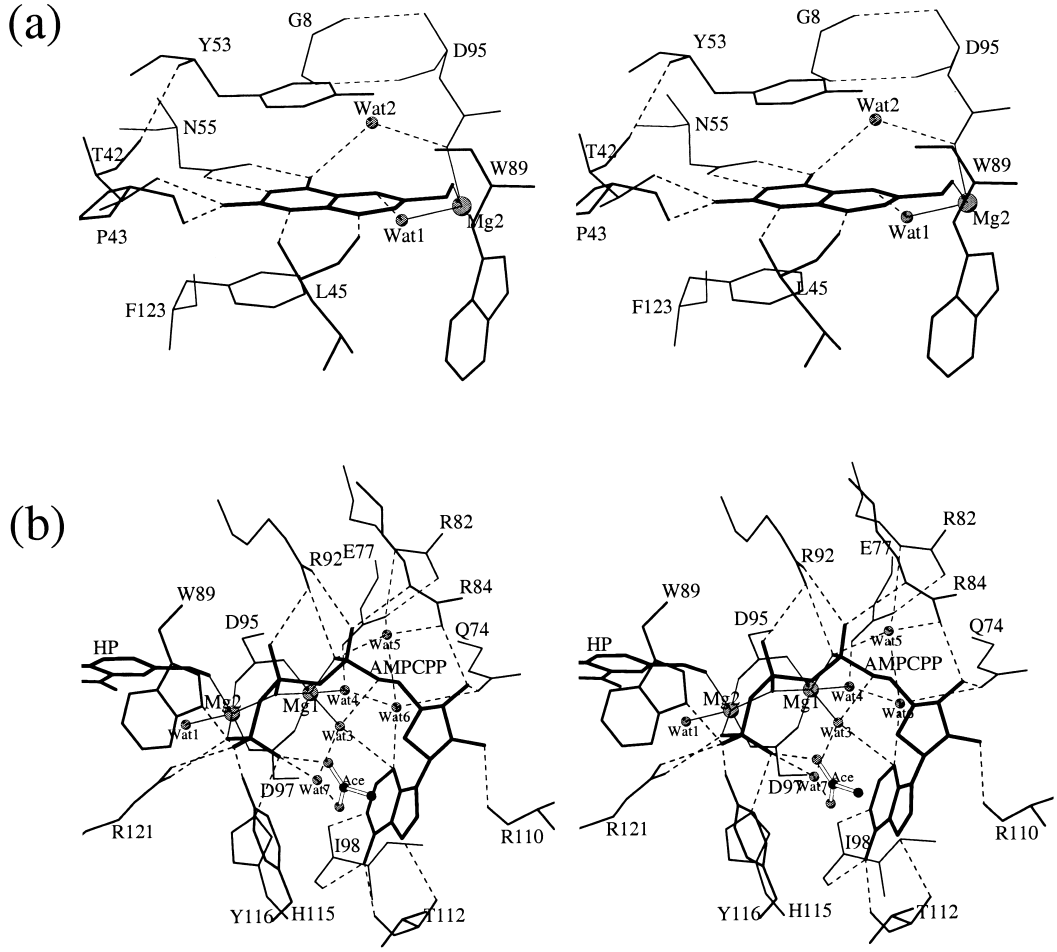

Figure 4. Stereoview of the amino acid residues (thin line) and water molecules within 5 Å of bound HP (a) and MgAMPCPP (b) (thick line). Water molecules and magnesium ions are shown as small and large balls respectively. The acetate ion is shown as a ball-and-stick model. Possible hydrogen bonds with donors and acceptors <3.5 Å apart are indicated by dashed lines. The coordination chemistry of the two bound magnesium ions is indicated by thin lines. The illustration was prepared using MOLSCRIPT.[22]

dramatic changes are the positional shifts of Leu45 and Trp89, of which the Cα atoms shift 4.8 and 7.9 Å, respectively. All the positional shifts are associated with the conformational changes of loops 2 and 3. The substrate-binding-induced fit of the HP-binding site is therefore obvious. The binding of the two Mg^{2+} ions requires significant conformational changes of Asp95 and Asp97, including an 80° rotation around the Cα-Cβ bond of Asp95 and a 70° rotation about the Cβ-Cγ bond of Asp97. Therefore, Mg^{2+}-binding-induced fit is also evident. The phosphate-bridge-binding pocket is formed in HPPK · HP · MgAMPCPP, whereas it is not seen in apo-HPPK. All three nucleotide-binding residues of Loop-3 (Arg84, Trp89, and Arg92) undergo dramatic positional shifts and conformational changes upon AMPCPP binding. In contrast, Gln74, Glu77, and Arg110 slightly change the conformation of their side chains, whereas Ile98, Thr112, Pro114, His115, Tyr116, and Arg121 do not show any significant difference. Arg88 in Loop-3 shifts with W89 upon substrate binding and forms a hydrogen bond with Tyr116, therefore contributing to the stabilization of the ternary complex. Arg88 also interacts with the ester oxygen between the β- and γ-phosphate groups via a water molecule. Of the active center of HPPK, only the adenine-binding pocket is rigid, which is responsible for the adenosine specificity of the enzyme. Conserved residues Leu111 and Pro114 contribute to the rigidity and stability of this region. Leu111 is packed with five other hydrophobic side chains (Pro66, Leu70, Leu98, Leu106, and Val113), and Pro114 is surrounded by Val105, Met118, Leu125, Phe137, and Leu138. Because of the adenosine specificity, the binding of MgATP is 260-fold higher than that of MgGTP and more than 1000-fold higher than those of other nucleoside triphosphates.[18] When no nucleotide is bound, four water molecules fill in the space and form the same hydrogen bond network with Ile98, Arg110, and Thr112.

Roles of Active-Site Residues

HPPK is a relatively small protein with 158 residues. Of the 158 residues, 26 residues are involved directly and indirectly in catalyzing the transfer of the pyrophosphate from ATP to HP. The crystal structures of apo-HPPK and HPPK · HP · MgAMPCPP have provided important clues on the functional

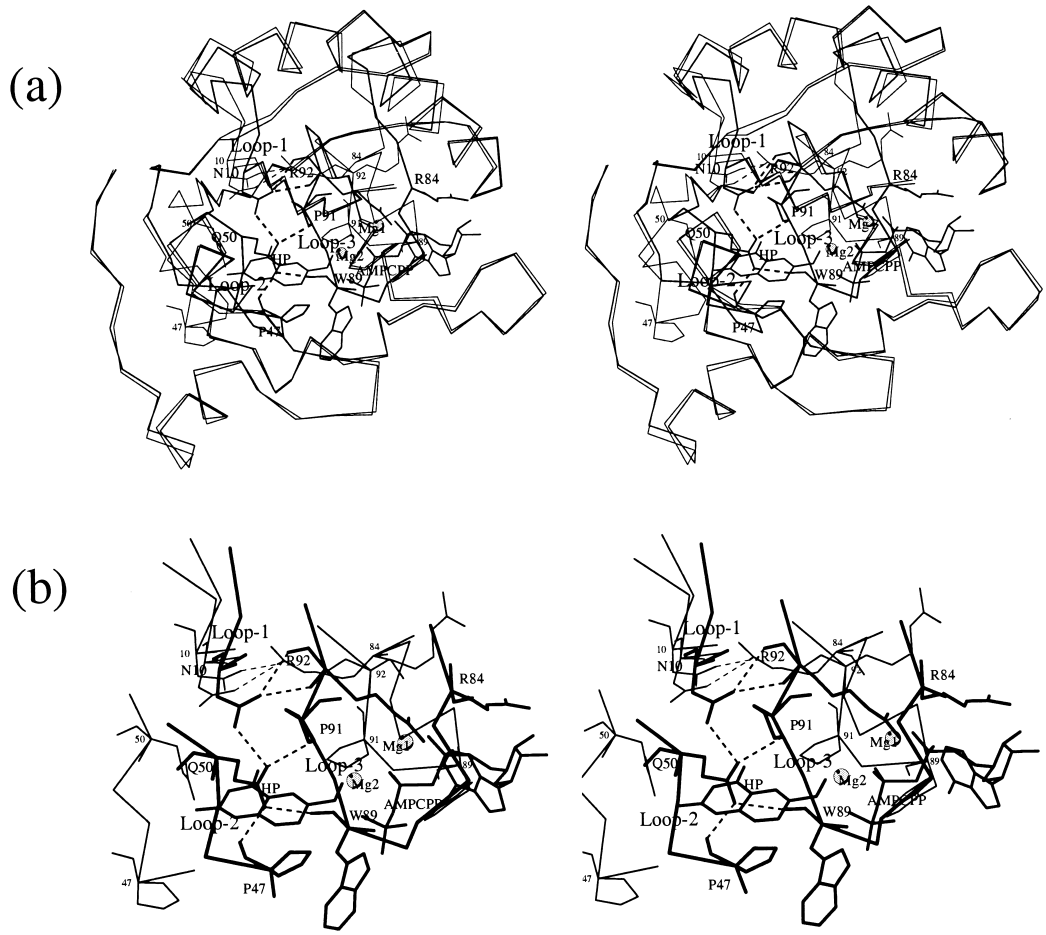

Figure 5. (a) Stereo view of the open and closed catalytic center of HPPK. The hydrogen bond network formed upon the binding of HP and MgAMPCPP is shown with the Cα-trace of HPPK · HP · MgAMPCPP (thick black line) superimposed with that of apo-HPPK (thin line). (b) A close-up of the hydrogen bond network formed upon the binding of HP and MgAMPCPP. The illustration was prepared using MOLSCRIPT.[22]

roles of these residues. Any mutation of the strictly conserved residue Gly8 will have two effects: it will prohibit the conformational change of Asn55 that is essential for HP binding, and it will inhibit HP binding directly via steric interactions. The conserved residues Asn10 and Gln50 form the center of a hydrogen bond network that couples all three flexible loops when the substrates are bound (Figure 5b). Asn55 readily recognizes HP and forms two hydrogen bonds with HP (Figure 4). The conformational change involved for Asn55-HP recognition and binding is only a 23° rotation about the Cα—Cβ bond of Asn55. Glu77 interacts with MgATP via water molecules and also keeps Arg82 in the vicinity through a salt-bridge. Arg92 has two functions: to participate in the formation of the hydrogen bond network that couples all three loops and to bind ATP. Asp95 and Asp97 are essential for coordinating the two Mg^{2+} ions for catalysis. Both Leu111 and Pro114 play important structural roles, being the center of hydrophobic cores of the protein. Leu111 packs together with five other hydrophobic side chains, including Pro66, Leu70, Leu98, Leu106, and Val113. Pro114 is surrounded by the side chains of Val105, Met118, Leu125, Phe137, and Leu138. The formation of these hydrophobic cores results in the rigidity of the adenine-binding pocket that is responsible for the nucleotide specificity of the enzyme. Both His115 and Arg121 interact with the γ-phosphate oxygen of bound ATP. Residues Pro43 and Leu45 form hydrogen bonds, with their amide and/or carbonyl groups, to HP (Figure 4), although dramatic positional shifts and conformational changes are involved. Tyr53 interacts with bound HP via its aromatic ring system and, therefore, a phenylalanine at this position is equally functional. Ile98, Arg110, and Thr112 interact with bound adenosine with their amide and/or carbonyl groups. Because the functional groups of Pro43, Leu45, Ile98, Arg110, and Thr112 are amides and carbonyls, the side chain variations at these positions should have no impact on their function. The nonconserved substrate-interacting residues are intriguing. They may be responsible for important differences for HPPK isozymes from different biological sources. Thr42 forms a hydrogen bond with HP using its atom OG (Figure 4), which is equivalent to the OG of a serine residue. Therefore, the interaction between this residue and HP is conserved for eight HPPKs. There are three variations (Figure 2), however, at this position, including lysine, asparagine, and alanine, which must cause significant differences in the structure and function of this residue. Gln74 forms a hydrogen bond with the ribose hydroxyl (Figure 4). Although Gln74 is conserved in five HPPKs, one phenylalanine, two

lysine, and three leucine residues are found in other isozymes (Figure 2). These residues, especially leucine and phenylalanine, have completely different properties. Therefore, different ATP-binding modes are expected for these two variants. Arg84 plays dual roles in *E. coli* HPPK. In the apo-enzyme, it forms a hydrogen bond with Asn10, even though Asn10 assumes two positions. The distances from NH2 of Arg84 to OD1 of N10 are 2.5 and 2.8 Å, respectively, for the two positions of Asn10. In the ternary complex, Arg84 interacts with both phosphate and ribose (Figure 4). It is conserved in eight HPPKs and is a lysine residue in two HPPKs (Figure 2). The only significant variation among 11 HPPKs is Asp84 at this position, which must have a significant impact on protein–ATP interaction and catalysis. For example, Asp84 may form salt bridges with both Arg82 and Arg92, which will play a negative role in ATP binding. Arg88 is conserved in six HPPKs, is a histidine residue in one and a lysine residue in three HPPKs, and is absent in one HPPK (Figure 2). In *E. coli* enzyme, it interacts with the oxygen bridge between the β- and γ-phosphates of bound ATP via a water molecule (Figure 4). More interestingly, via a hydrogen bond to the hydroxyl of Tyr116, Arg88 forms the edge of the sealed active center. Trp89 is conserved in seven HPPKs (Figure 2). Other variants at this position include tyrosine, aspartic acid, and two deletions. Trp89 in *E. coli* HPPK plays three roles. It participates in the formation of the hydrogen bond network between the loops, provides a hydrophobic interaction with bound HP, and forms a hydrogen bond with one of the γ-phosphate oxygen atoms. Variations at position 89 must result in distinct protein–substrate interactions. Tyr116 is even more interesting. In *E. coli* HPPK, it does not undergo a significant positional shift or conformational change upon substrate binding and is hydrogen bonded to both the γ-phosphate of ATP and the guanidinium group of Arg88 (Figure 4). In *H. influenzae* HPPK, however, Tyr116 points with its side chain to the opposite direction [16]. Yet, Tyr116 is conserved in only these two isozymes (Figure 2). Other variations include one arginine, one glutamic acid, and seven proline residues. Taking into account residues 88 and 116, the variations at these two positions give rise to the variation of the sealed active center, the biological impact of which may be significant. Phe123 is conserved in 10 HPPKs (Figure 2). The only exception is serine at this position. Because the functional group of Phe123 is its aromatic ring system, the serine variant must have a distinct HP binding mode, which remains to be elucidated.

PERSPECTIVES

Comparison of the crystal structures of apo-HPPK and HPPK · HP · MgAMPCPP has revealed dramatic conformational changes of three flexible loops and many side chains and possible roles of active site residues. Interestingly, binding of MgADP or MgAMPCPP induces a dramatic, unusual movement of loop 3 as revealed by the crystal structure of HPPK in complex with MgADP and the NMR solution structure of HPPK in complex with MgAMPPCP (Xiao et al., unpublished). Rather than moving in to close the active center of the enzyme as usually observed in substrate-induced fit, loop 3 moves away from the active center with some residues moving by >17 Å. The conformational changes may play important roles in facilitating both substrate binding and product release during the catalytic cycle. *E. coli* HPPK appears to be an excellent model for studying the roles and mechanisms of induced fit in catalysis because of the dramatic induced conformational changes and its friendliness to high resolution structural analysis. Clearly, more high-resolution structures of HPPK are needed to elucidate the induced conformational changes at each stage of the catalytic cycle. The roles of the amino acid residues involved in catalysis and induced fit need to be investigated by site-directed mutagenesis in conjunction with kinetic and structural analyses of the mutants.

ACKNOWLEDGMENT

This work was supported in part by NIH grant GM51901 awarded to H.Y.

REFERENCES

1 Cohen, M.L. Epideminology of drug resistance: implications for a post-antimicrobial era. *Science* 1992, **257**, 1050–1055
2 Neu, H.C. The crisis in antibiotic resistance. *Science* 1992, **257**, 1064–1072
3 Kunin, C.M. Resistance to antimicrobial drugs—a worldwide calamity. *Ann. Intern. Med.* 1993, **118**, 557–561
4 Levy, S.B. Antimicrobial resistance: A global perspective. *Ad. Exp. Med. Biol.* 1995, **390**, 1–15
5 Murray, B.E. Antibiotic resistance. *Ad. Intern. Med.* 1997, **42**, 339–367
6 World Health Organization. *World Health Organization Report on Infectious Diseases: Removing Obstacles to Healthy Development.* World Health Organization, Geneva, 1999
7 Shiota, T. Biosynthesis of folate from pterin precursors. In: *Chemistry and Biochemistry of Folates*, Blakley, R.T., and Benkovic, S.J., Eds., John Wiley & Sons, Inc., New York, 1984, Vol. 1, pp. 121–134
8 Blakley, R.L., and Benkovic, S.J., Eds. *Chemistry and Biochemistry of Folates.* Folates and Pterins. Vol. 1, John Wiley & Sons, Inc., New York, 1984
9 Hughes, D.T.D. Sulphonamides. In: *Antibiotic and Chemotherapy*, O'Grady, F., Lambert, H.P., Finch, R.G., and Greenwood, D., Eds., Churchill Livingstone, New York, 1997, pp. 460–468
10 Hughes, D.T.D. Diaminopyrimidines. In: *Antibiotic and Chemotherapy*, O'Grady, F., Lambert, H.P., Finch, R.G., and Greenwood, D., Eds., Churchill Livingstone, New York, 1997, pp. 346–356
11 Talarico, T.L., Dev, I.K., Dallas, W.S., Ferone, R., and Ray, P.H. Purification and partial characterization of 7,8-dihydro-6-hydroxymethylpterin-pyrophosphokinase and 7,8-dihydropteroate synthase from *Escherichia coli* MC4100. *J. Bacteriol.* 1991, **173**, 7029–32
12 Talarico, T.L., Ray, P.H., Dev, I.K., Merrill, B.M., and Dallas, W.S. Cloning, sequence analysis, and overexpression of *Escherichia coli folK*, the gene coding for 7,8-dihydro-6-hydroxymethylpterin-pyrophosphokinase. *J. Bacteriol.* 1992, **174**, 5971–7
13 Switzer, R.L. Phosphoribosylpyrophosphate synthetase and related pyrophosphokinases. In: *The Enzymes*, Boyer, P., Ed., Academic Press, New York, 1974, Vol. 10, pp. 607–629
14 Xiao, B., Shi, G., Chen, X., Yan, H., and Ji, X. Crystal Structure of 6-Hydroxymethyl-7,8-dihydropterin Pyro-

phosphokinase, a potential target for development of novel antimicrobial agents. *Structure* 1999, **7**, 489–496
15 Shi, G., Gao, J., and Yan, H. ^{1}H, ^{13}C and ^{15}N resonance assignments of *Escherichia coli* 6-hydroxymethyl-7,8-dihydropterin pyrophosphokinase and its complex with MgAMPPCP. *J. Biomol. NMR* 1999, **14**, 189–190
16 Hennig, M., Dale, G.E., D'Arcy, A., Danel, F., Fischer, S., Gray, C.P., Jolidon, S., Müller, F., Page, M.G.P., Pattison, P., and Oefner, C. The structure and function of the 6-hydroxymethyl-7,8-dihydropterin pyrophosphokinase from *Haemophilus influenzae*. *J. Mol. Biol.* 1999, **287**, 211–219
17 Stammers, D.K., Achari, A., Somers, D.O., Bryant, P.K., Rosemond, J., Scott, D.L., and Champness, J.N. 2.0 Å X-ray structure of the ternary complex of 7,8-dihydro-6-hydroxymethylpterinpyrophosphokinase from *Escherichia coli* with ATP and a substrate analogue. *FEBS Lett.* 1999, **456**, 49–53
18 Shi, G., Gong, Y., Savchenko, A., Zeikus, J.G., Xiao, B., Ji, X., and Yan, H. Dissecting the nucleotide binding properties of *Escherichia coli* 6-hydroxymethyl-7,8-dihydropterin pyrophosphokinase with fluorescent 3′(2)′-o-anthraniloyladenosine 5′-triphosphate. *Biochem. Biophys. Acta* 2000, **1478**, 289–299
19 Blaszczyk, J., Shi, G., Yan, H., and Ji, X. Catalytic center assembly of 6-hydroxymethyl-7,8-dihydropterin pyrophosphokinase as revealed by the crystal structure of a ternary complex at 1.25 Å resolution. *Structure Fold Des.* 2000, **8**, 1049–1058
20 Carson, M. Ribbons. *Methods Enzymol.* 1997, **277**, 493–505
21 Nicholls, A., Sharp, K.A., and Honig, B. Protein folding and association: insights from the interfacial and thermodynamic properties of hydrocarbons. *Proteins* 1991, **11**, 281–296
22 Kraulis, P.J. MOLSCRIPT: a program to produce both detailed and schematic plots of protein structures. *J. Appl. Crystallogr.* 1991, **24**, 946–950